

# Synthesis of Fluorescent DNA-Modified Polymer Nanoparticles for Use in a Highly Sensitive DNA Detection Assay

*Undergraduate Researchers*  
Sharan R. Srinivasan  
Northwestern University

Megan M. Boyle  
Saint Mary's College, South Bend, Indiana

*Faculty Mentor*  
SonBinh T. Nguyen  
Department of Chemistry  
Northwestern University

*Graduate Student Mentor*  
Brian R. Stepp  
Department of Chemistry  
Northwestern University

## Abstract

Polymer nanoparticles (PNPs) were formed from amphiphilic diblock copolymers consisting of a hydrophilic block with pendant polyethylene glycol tosylate (PEG-OTs) groups and a hydrophobic block with pendant terthiophene (TTT) groups. The resulting PNPs were characterized using dynamic light scattering (DLS) and transmission electron microscopy (TEM) to determine size, shape, and polydispersity. Following characterization, PNPs were functionalized with oligonucleotides, and the success of functionalization was verified by hybridization of the DNA-modified PNPs with complementary DNA-functionalized gold nanoparticles (GNPs). DNA-functionalized PNPs were then able to be used as probes in a three-strand DNA detection assay employing the fluorescent and electrochemical properties of the TTT group as a multifunctional signaling unit.

## Introduction

DNA detection is an important area of research due to its utility in clinical diagnostics and forensics. As genetic diseases are often caused by mutations in the genetic code, detection of specific mutated sequences in a patient's genes can indicate propensity to diseases. In addition, early detection of the presence of foreign genetic materials would alert doctors to pathogenic infections and allow for proactive treatments. DNA forensic studies could be accelerated by the use of a highly sensitive detection assay. In all of these applications, the desired target strands often exist only in trace amounts and must be amplified before they can be reliably detected. The last three decades have witnessed several innovations aimed at detecting oligonucleotides in low concentrations.

The current industry standard for DNA amplification, polymerase chain reaction (PCR), is a powerful tool that can enable the detection of a mere few sequences of DNA. The PCR method involves continuous replication of a target sequence of DNA, initially present at very low concentration, to a level where it can be easily detected. Since this strategy involves repetitive enzyme-based replication, however, it is not immune to mistakes and can take hours and frequently days to

sufficiently amplify the target sequence. The overall lab results can take up to a week — far too long if the incubation period for a disease is only a few days. To diagnose illnesses more quickly, it is imperative that disease-specific sequences of DNA can be accurately detected at very low concentrations and on a timely basis.

Presently, techniques to increase the sensitivity and efficiency in DNA detection assays are being explored in laboratories around the world. This research explores a new strategy by creating a probe-based, sequence-specific DNA assay that does not require a separate amplification step, potentially enabling detection of DNA levels at better than femtomolar range. Application of this methodology to DNA detection could yield results in much shorter time periods than current technologies.

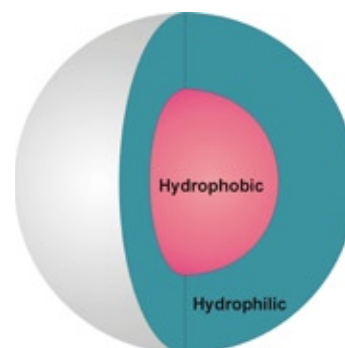
## Background

To detect a DNA strand, the molecular recognition event between a probe and this target strand must be paired with a signaling event that can be recognized by a macroscopic instrument. If the signaling event is based on a molecular probe, each successful binding event would lead only to a single molecular signal, which would be very difficult to assay in conventional settings. While recent innovation for detecting DNA has successfully coupled DNA-modified gold<sup>1</sup> and magnetic nanoparticles<sup>2</sup> to amplification processes, they necessitate extra modification steps. The purpose of this research is to synthesize a nanoparticle possessing an intrinsically amplified signal that allows for the elimination of such modifications. Such an accomplishment should greatly enhance DNA detection.

## Approach

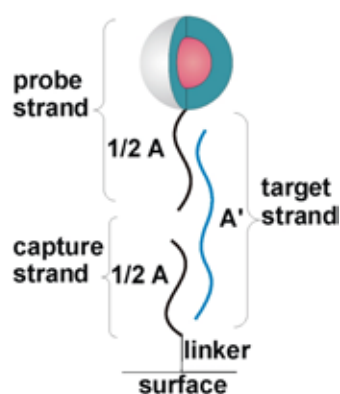
Polymer nanoparticles (PNPs) are formed from diblock copolymers that contain a biocompatible hydrophilic poly(ethylene glycol tosylate) (PEG-OTs) block as well as a multifunctional hydrophobic terthiophene (TTT) block. In aqueous media, these amphiphilic polymers assemble into micelle-like particles possessing a hydrophobic core consisting of TTT blocks and a hydrophilic corona made up from the PEG-OTs blocks (Figure 1). This arrangement exposes the terminal tosylate groups for future reaction with amine-terminated DNA to yield DNA-modified PNPs.<sup>3</sup> Once the PNPs have been successfully

**Figure 1.** A schematic diagram of a core-shell polymer nanoparticle (PNP).



assembled, they can be used in a three-strand “sandwich” assay (Figure 2) for detecting target oligonucleotides of known sequences in solution. In this scheme, the PNP is functionalized with amine-terminated DNA probe strands that are complementary to one end of the target DNA sequence, making one half of the “sandwich.” The other half is composed of a glass slide that has been modified with capture strands that are complementary to the other end of the target. If the target DNA sequence is present in a media containing both halves of the sandwich, it will hybridize together with the probe and capture strands and anchor the PNPs to the glass surface. An aqueous wash removes any unbound PNPs, and subsequent exposure of the PNP-bound slide to organic solvents will release the TTT blocks to serve as the signaling unit, allowing for convenient signal detection by both fluorometry and cyclic voltammetry.<sup>4</sup>

**Figure 2.** A schematic illustration of a three-strand detection assay.



## Materials

All solvents and reagents, with the exception of reagents for DNA synthesis, were purchased from the Aldrich Chemical Company and used as received. DNA strands were synthesized on an ABI 8909 Expedite Nucleic Acid Synthesis System with reagents purchased from Glen Research. Nanopure water was obtained from a Millipore system (18.2 M $\Omega$  cm resistivity).

## Instrumentation

Fluorescence spectra were obtained on a Jobin Yvon-SPEX Fluorolog fluorometer ( $\lambda_{\text{ex}} = 470$  nm,  $\lambda_{\text{em}} = 514$  nm). Cyclic voltammetry (CV) data were acquired on a CHI900 scanning electrochemical microscope using a conventional three-electrode cell (Pt disk working electrode, Ag/AgCl reference electrode, and Pt wire counter electrode). Transmission electron microscopy (TEM) work was performed on an Hitachi H8100 microscope operating at an accelerating voltage of 200 kV.

Static light-scattering (SLS) experiments were performed on a DAWN-EOS multiangle laser photometer (Wyatt Technology, Santa Barbara, California) equipped with an He-Ne laser (632.8 nm). Dynamic light-scattering (DLS) measurements were performed on a Brookhaven Instruments Corp. photon correlation spectrometer (BI-200 SM goniometer) fitted with a Brookhaven Instruments BI-9000AT digital correlator and a 3 W argon-ion laser delivering monochromatic light of 514.5 nm at a scattering angle of 90°. A bath of filtered decalin (0.2 m) surrounded the scattering cell, and the temperature was fixed at 25° C. Data for each sample were collected on a continuous basis for 2 min in sets of three. Based on the scattered light intensity of the solution, the average diameter of the particles and the monodispersity are calculated and given as the polydispersity index (PDI). A PDI of zero equates to a completely homogenous sample.

Polymer molecular weights were measured relative to polystyrene standards on a Waters gel-permeation chromatograph (GPC) equipped with Breeze software, a 717 autosampler, Shodex KF-G guard column, KF-803L and KF-806L columns in series, a Waters 2440 UV detector, and a 410 RI detector. HPLC-grade THF was used as the eluent at a flow rate of 1.0 mL/min, and the instrument was calibrated using polystyrene standards (Aldrich, 15 standards, 760-1,800,000 Daltons). A PDI of 1.0 is indicative of a monodisperse polymer sample.

## Results and Discussion

### Synthesis and Properties of Polymers

Tosylated norbornene-modified hexaethylene glycol and norbornene-modified terthiophene were synthesized using reported literature procedures<sup>3,5</sup> (Figure 3) and subsequently polymerized via ring-opening metathesis polymerization (ROMP) (Figure 4). The molecular weight and PDI of the synthesized block polymers were determined by gel-permeation chromatography (GPC). The data in Table 1 indicate that nearly all the polymers can be made with a sufficiently low polydispersity for productive PNP formation (see next page).

Before PNP synthesis, it was necessary to prove that the TTT block of the copolymers possessed both fluorescent and electrochemical behaviors suitable for use in detection. Figure 5 displays plots of the fluorescence intensity vs. the fluorophore concentration for both free terthiophene and TTT<sub>40</sub>-b-(PEG-OTs)<sub>15</sub> copolymer. These two plots are quite similar in their concentration dependencies, suggesting that attachment of terthiophene to the polymer backbone does not significantly affect its fluorescent behavior. As expected, the maximum fluorescence of the terthiophene fluorophores generally increases with increased concentration. However, the increase is not uniformly linear — the dependence between 10<sup>-10</sup> to 10<sup>-15</sup> M is less pronounced than that between 10<sup>-6</sup> to 10<sup>-15</sup> M. Interestingly, as the terthiophene concentration increases above 10<sup>-7</sup> M, there is a significant drop in the fluorescence intensity. This is presumably due to proximity-induced self-quenching — as the fluorophore reaches a certain threshold concentration, the molecules become so close to one another that the energy emitted by one molecule is immediately absorbed by its neighbor and the emission signal is diminished.

The electrochemical data for the polymer are displayed in Figure 6. While the cyclic voltammetry curve shows detectable mA-level current down to the femtomolar concentration, linearity was observed only down to micromolar concentrations. Unlike fluorescence, no self-quenching occurs in electrochemistry, and the limitation for current detection is bound only by the size of the electrode. Although the current electrochemical data do not show the same sensitivity as the fluorometry data, using microelectrodes should lead to much improved analyte response. In addition, incorporation of electrochemical readouts into an assay would be much easier and less expensive to implement than the corresponding fluorescent analogs.

While the plots of Figures 5 and 6 indicate that readout signals can be obtained even at femtomolar concentration, these readings may not be reliable at such low concentrations due to the limitations of the instrument. It is noted that the general increase of fluorescence intensity and oxidation current with increased terthiophene concentration should, in theory, provide an opportunity for quantifying the amount of a target DNA strand. However, this would require significant investment in mapping out a calibration that includes the concentration of the OTs groups on the PNP surface, the density of capture strands, the size of the PNP, the kinetics of the capture process, and the solution concentrations of analyte/PNPs.

# Synthesis of Fluorescent DNA-Modified Polymer Nanoparticles for Use in a Highly Sensitive DNA Detection Assay *(continued)*

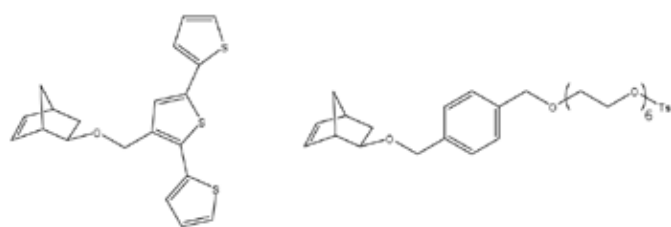


Figure 3. PEG-OTs and TTT monomers.

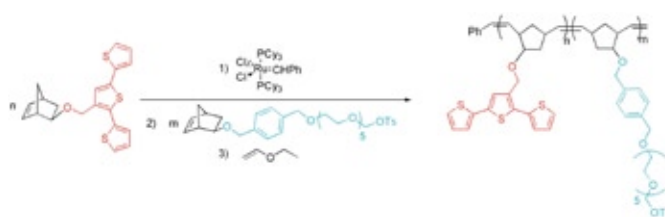


Figure 4. The synthesis of TTT<sub>n</sub>-b-(PEG-OTs)<sub>m</sub> polymers.

Trial	First monomer block	Amount of 1 <sup>st</sup> monomer used (mmol)	Second monomer block	Amount of 2 <sup>nd</sup> monomer used (mmol)	Amount of Grubb's catalyst (mmol)	Polydispersity index (PDI)
1	(PEG-OTs) <sub>15</sub> 1	25	TTT <sub>30</sub>	250	8.33	1.13
2	(PEG-OTs) <sub>15</sub> 1	18	TTT <sub>30</sub>	236	7.87	1.46
3	TTT <sub>30</sub> 1	85	(PEG-OTs) <sub>15</sub>	92.5	6.17	1.09
4	TTT <sub>40</sub> 2	47	(PEG-OTs) <sub>15</sub>	92.5	6.17	1.10
5	TTT <sub>45</sub> 2	38	(PEG-OTs) <sub>15</sub>	79.3	5.29	1.10
6	TTT <sub>50</sub> 3	08	(PEG-OTs) <sub>15</sub>	92.5	6.17	1.10

Table 1. Polymerizations and conditions.

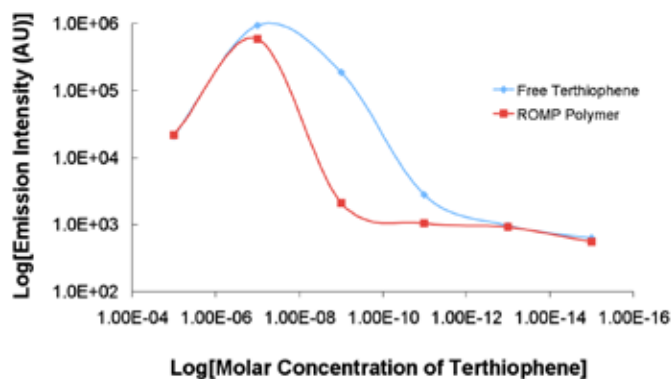


Figure 5. Plots of fluorescence intensity vs. chromophore concentration for free terthiophene and TTT<sub>40</sub>-b-(PEG-OTs)<sub>15</sub>.

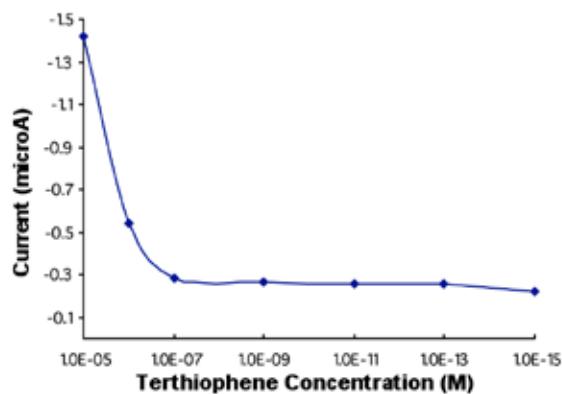
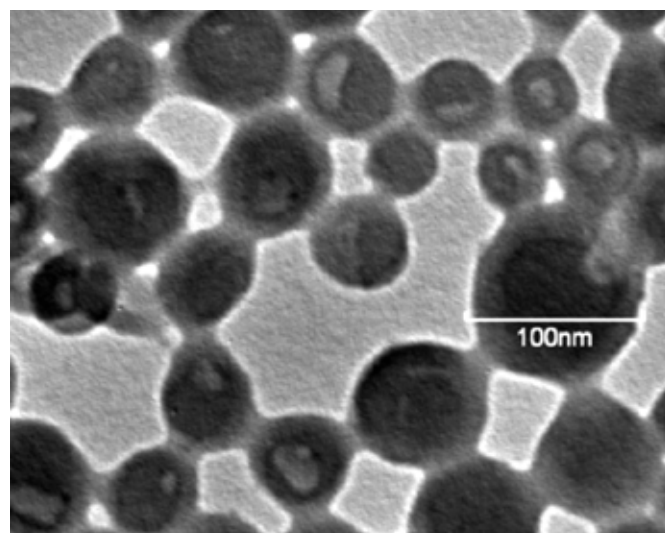


Figure 6. Plot of oxidation current vs. terthiophene concentration for TTT<sub>40</sub>-b-(PEG-OTs)<sub>15</sub>.

Polymer	Wt%	Solvent	CWC (vol%)	Total water added (vol%)	Diameter (DLS) (nm)	PDI (DLS)
TTT <sub>30</sub> - <i>b</i> -(PEG-OTs) <sub>15</sub> <sup>a</sup> 0	.010 D	MF	1.2	12.79	185	0.05
TTT <sub>30</sub> - <i>b</i> -(PEG-OTs) <sub>15</sub> 0	.010 T	HF N	/A 4	3.70 5	00 0	.17
TTT <sub>40</sub> - <i>b</i> -(PEG-OTs) <sub>15</sub> 0	.010 D	MF	1.0	13.20	125	0.05
TTT <sub>40</sub> - <i>b</i> -(PEG-OTs) <sub>15</sub> 0	.005 D	MF	1.5	14.50	280	0.05
TTT <sub>40</sub> - <i>b</i> -(PEG-OTs) <sub>15</sub> <sup>a</sup> 0	.010 D	MF	2.2	14.29	240	0.10
TTT <sub>40</sub> - <i>b</i> -(PEG-OTs) <sub>15</sub> 0	.010 T	HF N	/A 5	6.52 1	20 0	.15
TTT <sub>45</sub> - <i>b</i> -(PEG-OTs) <sub>15</sub> 0	.010 T	HF 2	7.9	33.90	1000 0	.01
TTT <sub>45</sub> - <i>b</i> -(PEG-OTs) <sub>15</sub> 0	.010 D	MF	0.7	13.29	270	0.15
TTT <sub>45</sub> - <i>b</i> -(PEG-OTs) <sub>15</sub> <sup>a</sup> 0	.010 D	MF	.4 1	8.83 2	50 0	.12

<sup>a</sup> indicates the sample was heated near the critical water content

**Table 2.** Data for the preparation of PNP.



**Figure 7.** TEM image of nanoparticles assembled from TTT<sub>40</sub>-*b*-(PEG-OTs)<sub>15</sub> copolymer.

#### PNP Formations

Formation of PNPs involves the slow addition of water (25  $\mu$ L every minute) to a dilute solution (0.01 M) of the copolymer in a water-miscible organic solvent. The process can be monitored readily by static light scattering (SLS). When the critical water content (CWC) of the copolymer solution is reached (~30–40 vol% of added water), a sudden and significant increase in the intensity of scattered light occurs (the solution can become significantly cloudy), signifying nanoparticle formation.<sup>6,7</sup> Approximately 15–20 vol% of water was added past the CWC (also at 25  $\mu$ L every minute), and the particle suspensions were dialyzed to remove all the organic solvents following a method developed by Eisenberg and coworkers.<sup>8,9</sup> The PNPs thus formed were kept in deionized water for further analysis by DLS to determine average PNP diameter and the PDI (Table 2).

As determined by both DLS and TEM, the dispersity and diameter of PNP varied greatly in polymer weight percent, polymer composition, and technique. The weight percent that appeared to work the best was 0.01, although 0.005 did give consistent particles that were a bit larger

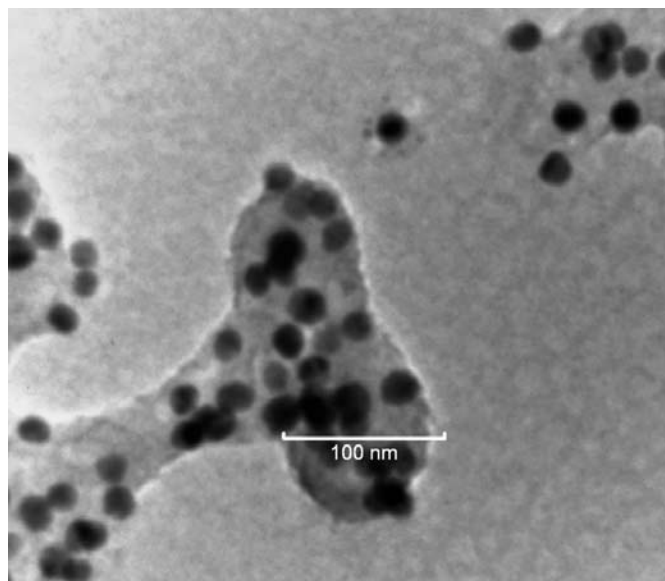


**Figure 8.** TEM image of DNA-functionalized PNP exposed to 13 nm GNPs possessing complementary DNA strands.

(Table 2). Following experimentation with a few polymer compositions, the TTT<sub>45</sub>-b-(PEG-OTs)<sub>15</sub> copolymer seemed to provide the most consistent PNPs (Figure 7). Copolymers having low PDIs often result in more stable monodisperse PNPs. As seen in Table 2, PNP formation does not follow a clear solvent trend, and it is suspected that it is quite technique dependent, especially regarding the frequency, rate, and amount of water addition.

Once ideal PNP formation conditions were determined, PNPs were incubated with amine-terminated DNA. The success of this modification was verified by exposing the DNA-functionalized PNP to solutions of gold nanoparticles (GNPs)<sup>9</sup> that were prefunctionalized with either complementary or noncomplementary DNA strands and viewing the results using TEM. In the first case, the smaller GNPs appeared as black dots embedded all over the larger PNPs, signifying a proper hybridization of the GNPs to the DNA-modified PNPs (Figure 8). In the second case, although the GNPs appeared close to the PNPs (Figure 9), they were not embedded in the PNPs, suggesting nonspecific binding that was a result of particle aggregation as the sample dried. Together, these results indicated that the PNPs do possess surface OTs groups that can be readily modified with amine-functionalized DNA.

The PNPs in Figures 8 and 9 appeared to lose their spherical shapes after modification. This lack of stability suggests a need for more stable

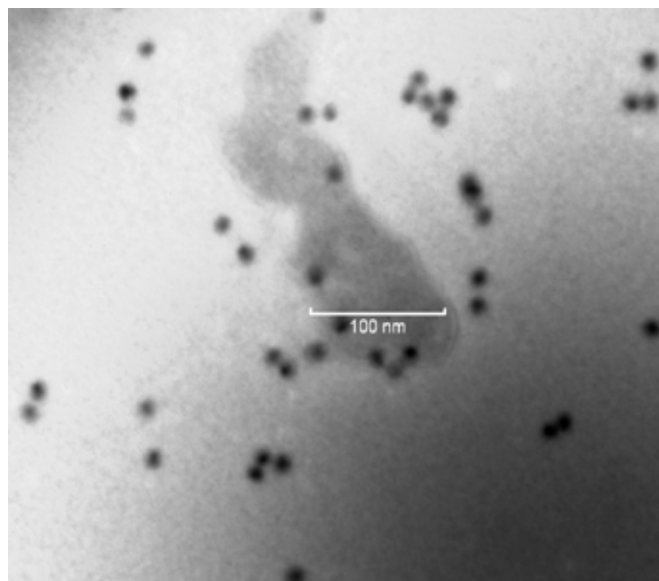


**Figure 9.** TEM image of DNA-functionalized PNP exposed to 13 nm GNPs possessing noncomplementary DNA strands.

PNPs, possibly via other polymer compositions, before this system can be incorporated into a practical DNA detection. Future attempts will include using a more hydrophobic copolymer such as TTT<sub>60</sub>-b-(PEG-OTs)<sub>15</sub>. The longer hydrophobic block should result in a tightly packed core and more stable PNPs that can withstand subsequent DNA hybridization chemistry as well as integration into a practical DNA detection system.

### Conclusion

In an attempt to develop a highly sensitive methodology for the detection of low concentrations of DNA, a promising polymer probe was synthesized that should allow for facile visualization through either electrochemistry or fluorescence. While such amphiphilic polymers can be assembled into PNPs and functionalized with DNAs, they are not stable enough to be incorporated into a detection system. Future work will emphasize the synthesis of nanoparticles with better stability as well as implementation of such particles into a three-strand DNA assay.

*This research was supported primarily by the Nanoscale Science and Engineering Initiative of the National Science Foundation under NSF award number EEC-0647560. Any opinions, findings, and conclusions or recommendations expressed in this material are those of the authors and do not necessarily reflect those of the National Science Foundation.*

### References

- 1 Elghanian, R.; Storhoff, J. J.; Mucic, R. C.; Letsinger, R. L.; Mirkin, C. A. *Science* **1997**, *277*, 1078–1081.
- 2 Stoeva, S. I.; Lee, J.; Thaxton, C. S.; Mirkin, C. A. *Angew. Chem. Int. Ed.* **2006**, *45*, 3303–3306.
- 3 Bertin, P. A.; Gibbs, J. M.; Shen, C. K.; Thaxton, C. S.; Russin, W. A.; Mirkin, C. A.; Nguyen, S. T.; *J. Am. Chem. Soc.* **2006**, *128*, 4168–4169.
- 4 Gratzl, M.; Hsu, D.; Riley, A. M.; Janata, J. *J. Phys. Chem.* **1990**, *94*, 5973–5981.
- 5 Watson, K. J.; Wolfe, P. S.; Nguyen, S. T.; Zhu, J.; Mirkin, C. A. *Macromolecules* **2000**, *33*, 4628–4633.
- 6 Zhang, L.; Eisenberg, A.; *Polym. Adv. Technol.* **1998**, *9*, 677–699.
- 7 Storhoff, J. J.; Elghanian, R.; Mucic, R. C.; Mirkin, C. A.; Letsinger, R. L. *J. Am. Chem. Soc.* **1998**, *120*(9), 1959–1964.
- 8 Li, Z.; Zhao, W.; Liu, Y.; Rafailovich, M. H.; Sokolov, J.; Khougaz, K.; Eisenberg, A.; Lennox, R. B.; Krausch, G.; *J. Am. Chem. Soc.* **1996**, *118*, 10892–10893.
- 9 Gao, Z.; Varshney, S. K.; Wong, S.; Eisenberg, A. *Macromolecules* **1994**, *27*, 7923–7927.
- 10 Wu, Z.; Jiang, J.; Fu, L.; Shen, G.; Yu, R. *Anal. Biochem.* **2006**, *353*, 22–29.